

Video Article

Recording Brain Electromagnetic Activity During the Administration of the Gaseous Anesthetic Agents Xenon and Nitrous Oxide in Healthy Volunteers

Andria Pelentritou¹, Levin Kuhlmann¹, John Cormack², Will Woods³, Jamie Sleigh⁴, David Liley¹

¹Centre for Human Psychopharmacology, Swinburne University of Technology

²Department of Anaesthesia and Pain Management, St. Vincent's Hospital Melbourne

³Brain and Psychological Science Research Centre, Swinburne University of Technology

⁴Department of Anaesthesiology, University of Auckland

Correspondence to: David Liley at dliley@swin.edu.au

URL: <https://www.jove.com/video/56881>

DOI: [doi:10.3791/56881](https://doi.org/10.3791/56881)

Keywords: Neuroscience, Issue 131, Magnetoencephalography, Electroencephalography, Anesthesia, Xenon, Nitrous Oxide

Date Published: 1/13/2018

Citation: Pelentritou, A., Kuhlmann, L., Cormack, J., Woods, W., Sleigh, J., Liley, D. Recording Brain Electromagnetic Activity During the Administration of the Gaseous Anesthetic Agents Xenon and Nitrous Oxide in Healthy Volunteers. *J. Vis. Exp.* (131), e56881, doi:10.3791/56881 (2018).

Abstract

Anesthesia arguably provides one of the only systematic ways to study the neural correlates of global consciousness/unconsciousness. However to date most neuroimaging or neurophysiological investigations in humans have been confined to the study of γ -Amino-Butyric-Acid-(GABA)-receptor-agonist-based anesthetics, while the effects of dissociative N-Methyl-D-Aspartate-(NMDA)-receptor-antagonist-based anesthetics ketamine, nitrous oxide (N_2O) and xenon (Xe) are largely unknown. This paper describes the methods underlying the simultaneous recording of magnetoencephalography (MEG) and electroencephalography (EEG) from healthy males during inhalation of the gaseous anesthetic agents N_2O and Xe. Combining MEG and EEG data enables the assessment of electromagnetic brain activity during anesthesia at high temporal, and moderate spatial, resolution. Here we describe a detailed protocol, refined over multiple recording sessions, that includes subject recruitment, anesthesia equipment setup in the MEG scanner room, data collection and basic data analysis. In this protocol each participant is exposed to varying levels of Xe and N_2O in a repeated measures cross-over design. Following relevant baseline recordings participants are exposed to step-wise increasing inspired concentrations of Xe and N_2O of 8, 16, 24 and 42%, and 16, 32 and 47% respectively, during which their level of responsiveness is tracked with an auditory continuous performance task (aCPT). Results are presented for a number of recordings to highlight the sensor-level properties of the raw data, the spectral topography, the minimization of head movements, and the unequivocal level dependent effects on the auditory evoked responses. This paradigm describes a general approach to the recording of electromagnetic signals associated with the action of different kinds of gaseous anesthetics, which can be readily adapted to be used with volatile and intravenous anesthetic agents. It is expected that the method outlined can contribute to the understanding of the macro-scale mechanisms of anesthesia by enabling methodological extensions involving source space imaging and functional network analysis.

Video Link

The video component of this article can be found at <https://www.jove.com/video/56881/>

Introduction

There is good consensus between pre-clinical and clinical neuroscientific evidence suggesting that the phenomenon of human consciousness depends on the integrity of explicit neural circuits. The observation that such circuits are systematically influenced by the descent into unconsciousness has substantiated the need for neuroimaging techniques to be utilized during anesthesia and enable 'navigating' the search for the neural correlates of consciousness. With the possible exception of sleep, anesthesia represents the only method by which one can, in a controlled, reversible and reproducible fashion, perturb, and thus dissect, the mechanisms that sub-serve consciousness, especially at the macroscopic scale of global brain dynamics. Clinically, general anesthesia can be defined as a state of hypnosis/unconsciousness, immobility and analgesia and remains one of the most abundantly used and safest medical interventions. Despite the clarity and efficiency in the end result, there remains great uncertainty regarding the mechanisms of action of the various types of agents giving rise to anesthetic induced unconsciousness¹.

Anesthetics can be divided into intravenous agents notably propofol and the barbiturates, or volatile/gaseous agents such as sevoflurane, isoflurane, nitrous oxide (N_2O) and xenon (Xe). The pharmacology of anesthesia has been well established with multiple cellular targets identified as linked to anesthetic action. Most agents studied to date act principally via the agonism of γ -Amino-Butyric-Acid-(GABA) receptor mediated activity. In contrast, the dissociative agents ketamine, Xe and N_2O are believed to exert their effects by primarily targeting N-Methyl-D-Aspartate-(NMDA) glutamatergic receptors^{2,3}. Other important pharmacological targets include potassium channels, acetylcholine receptors and the remnant glutamate receptors, AMPA and kainate, however the extent of their contribution to anesthetic action remains elusive (for a comprehensive review see ⁴).

The extent of variability in the mechanism of action and the observed physiological and neural effects of the various types of agents renders the derivation of general conclusions on their influence on conscious processing difficult. Loss of consciousness (LOC) induced by GABAergic agents is typically characterized by a global change in brain activity. This is evident in the emergence of high-amplitude, low-frequency delta (δ , 0.5–4 Hz) waves and the reduction in high frequency, gamma (γ , 35–45 Hz) activity in the electroencephalogram (EEG), similar to slow wave sleep^{5,6} as well as the widespread reductions in cerebral blood flow and glucose metabolism^{5,6,7,8,9,10,11,12}. Boveroux *et al.*¹³ added to such observations by demonstrating a significant decrease in resting state functional connectivity under propofol anesthesia using functional magnetic resonance imaging (fMRI). In contrast, dissociative anesthetics yield a less clear profile of effects on brain activity. In some cases, they are associated with increases in cerebral blood flow and glucose metabolism^{14,15,16,17,18,19,20,21} while studies by Rex and colleagues²² and Laitio and colleagues^{23,24} looking at the effects of Xe provided evidence of both increased and decreased brain activity. A similar irregularity can be seen in the effects on the EEG signals^{25,26,27,28}. Johnson *et al.*²⁹ demonstrated an increase in total power of the low frequency bands delta and theta as well as in the higher frequency band gamma in a high density EEG study of Xe anesthesia while opposing observations were made for N₂O in the delta, theta and alpha frequency bands^{30,31} and for Xe in the higher frequencies³². Such variability in the effects of Xe on the electrical scalp activity can be observed in the alpha and beta frequency ranges also with both increases³³ and reductions³⁴ being reported.

In spite of the discrepancies mentioned above, the picture starts to become more consistent across agents when one attempts to look at alterations in functional connectivity between brain areas. Such measures however, have been predominantly restricted to modalities that necessarily make concessions with respect to either spatial or temporal resolution. While studies using the EEG appear to reveal clear, and to some extent consistent, changes in the topological structure of functional networks during anesthesia/sedation with propofol³⁵, sevoflurane³⁶ and N₂O³⁷, the widely spaced sensor level EEG data has insufficient spatial resolution to meaningfully define and delineate the vertices of the corresponding functional networks. Conversely, studies utilizing the superior spatial resolution of fMRI and positron emission tomography (PET), find similar topological alterations in large-scale functional connectivity to that of EEG^{13,38,39,40,41}, however possess insufficient temporal resolution to characterize phase-amplitude coupling in the alpha (8–13 Hz) EEG band and other dynamical phenomena that are emerging as important signatures of anesthetic action^{12,42}. Moreover, these measures do not directly evaluate electromagnetic neural activity⁴³.

Therefore, in order to meaningfully advance the understanding of the macroscopic processes associated with the action of anesthetics, the limitations of the previously mentioned investigations need to be addressed; the restricted coverage of anesthetic agents and the insufficient spatio-temporal resolution of the non-invasive measurements. On this basis, the authors outline a method to simultaneously record magnetoencephalogram (MEG) and EEG activity in healthy volunteers that has been developed for the administration of the gaseous dissociative anesthetic agents, Xe and N₂O.

The MEG is utilized as it is the only non-invasive neurophysiological technique other than the EEG that has a temporal resolution in the millisecond range. EEG has the problem of blurring of electrical fields by the skull, which acts as a low-pass filter on cortically generated activity, while MEG is much less sensitive to this issue and the issue of volume conduction⁴⁴. It can be argued that MEG has higher spatial and source localization accuracy than EEG^{45,46}. EEG does not allow true reference-free recording^{37,47}, however MEG does. MEG systems also typically record cortical activity in a much wider frequency range than EEG, including high gamma⁴⁸ (typically 70–90 Hz), which have been suggested to be involved in the hypnotic effects of anesthetic agents including Xe²⁹ and N₂O²⁸. The MEG offers neurophysiological activity that compliments that conveyed by EEG, as EEG activity relates to extracellular electrical currents whereas MEG mainly reflects the magnetic fields generated by intracellular currents^{46,49}. Furthermore, MEG is particularly sensitive to electrophysiological activity tangential to the cortex, while EEG mostly records extracellular activity radial to the cortex⁴⁹. Thus combining MEG and EEG data has super-additive advantages⁵⁰.

The gaseous dissociative agents Xe and N₂O have been chosen for the following principle reasons: they are odorless (Xe) or essentially odorless (N₂O) and thus can easily be utilized in the presence of control conditions when employed at sub-clinical concentrations. In addition, they are well suited for remote administration and monitoring in a laboratory environment due to their weak cardio-respiratory depressant effects⁶¹. Xenon and to a lesser extent N₂O, retain a relatively low minimum-alveolar-concentration-(MAC)-awake at which 50% of patients become unresponsive to a verbal command with values of $32.6 \pm 6.1\%$ ⁵¹ and $63.3 \pm 7.1\%$ ⁵² respectively. Despite Xe and N₂O both being NMDA receptor antagonists, they modulate the EEG differently - Xe appears to behave more like a typical GABAergic agent when monitored using the Bispectral Index^{33,53,54} (one of several approaches used to electroencephalographically monitor depth of anesthesia). In contrast, N₂O produces a much less apparent electroencephalographic effect in that it is poorly, if at all, monitored using the Bispectral Index²⁶. Because Xe has different reported electroencephalographic properties to the other dissociative agents, but possesses similar characteristics to the more commonly studied GABAergic agents, its electrophysiological study has the potential to reveal important features relating to the neural correlates of consciousness and the corresponding functional network changes. Agents that act at the NMDA receptor are likely to reveal more about the brain networks that subserve normal and altered consciousness, given the critical role that NMDA receptor mediated activity plays in learning and memory and its implicated role in a range of psychiatric disorders that include schizophrenia and depression⁸⁰.

This paper focuses primarily on the demanding and complex data collection procedure associated with the delivery of gaseous anesthetic agents in a non-hospital environment while simultaneously recording MEG and EEG. Basic data analysis at the sensor level is outlined and example data are provided illustrating that high-fidelity recordings can be obtained with minimal head movement. The many potential methods for subsequent source imaging and/or functional connectivity analysis that would be typically performed using this kind of data are not described, as these methods are well described in the literature and demonstrate various options for analysis^{55,56}.

Protocol

The study entitled "Effects of inhaled Xe and N₂O on brain activity recorded using EEG and MEG" was approved (approval number: 260/12) by the Alfred Hospital and Swinburne University of Technology Ethics Committee and met the requirements of the National Statement on Ethical Conduct in Human Research (2007).

1. Participant Selection and Pre-Study Requirements

1. Conduct an interview to select healthy, right handed, adult males between the ages of 20 and 40 years old.

1. Confirm a good general health status by obtaining the participant's Body Mass Index (BMI) and the lack of contraindications to MRI or MEG (such as implanted metallic foreign bodies), as well as collecting a detailed medical history including any previous surgeries, importantly any unfavorable reactions to general anesthesia which would result in exclusion from the study.
2. Specifically exclude any recent intake of psychoactive or other prescribed medication as well as ensuring the absence of any recreational drug use and the lack of any neurological disorder, epilepsy, heart conditions, sleep apnea, motion sickness and claustrophobia. As it will be subsequently important to obtain a good seal with an anesthetic face mask exclude participants who have large beards, unless they are willing to shave.
NOTE: Exclude females due to the documented effects of menstruation⁵⁷ and/or age extremes on the resting MEG/EEG signal as well as the increased propensity to nausea and vomiting⁵⁸.
2. Follow the day stay general anesthesia procedure as designated in the Australia and New Zealand College of Anaesthetists (ANZCA) guidelines (Document PS15).
 1. In line with these guidelines, ask the subjects to fast for at least 6 hours and consume no liquids for at least 2 hours prior to the start of the experiment. Confirm compliance by having the anesthesiologist contacting the participant the day before the testing takes place.
 2. After the completion of the experiment, have subjects undergo standard post anesthesia care monitoring by instructing them not to operate any heavy machinery or make important decisions within 24 hours of the experiment (due to the possibility of residual low level cognitive impairment from Xe and N₂O).

2. Facilities and Equipment

NOTE: The facilities are in accordance with ANZCA requirements for the delivery of anesthesia outside a normal surgical operating suite (<http://www.anzca.edu.au/resources/professional-documents>. Document PS55). Specifically, the room satisfies engineering regulations for electrical safety and gas medical administration.

1. Run the experiment at the Swinburne Advanced Technology Centre's Brain Imaging laboratory, namely the MEG room which contains a magnetically shielded room (MSR) that houses the MEG scanner. The shielded room sits on a floating floor isolated from environmental movements such as passing trains.
2. Deliver anesthesia gases using an anesthesia machine, located outside the MSR, capable of delivery and monitoring gaseous xenon. This anesthesia machine is specially designed to administer closed-loop low flow Xe gas and to measure end-tidal Xe concentrations using katharometry (thermal conductivity; $\pm 1\%$ accuracy), in addition to providing standard-of-care patient monitoring. This includes end-tidal O₂, CO₂, N₂O measurement (where appropriate), pulse oximetry, 3-lead ECG, and non-invasive blood pressure measurement (NIBP) as per ANZCA Guideline Document PS18. Measure end-tidal N₂O concentrations using infrared spectroscopy implemented in the anesthesia machine.
 1. Pipe the gases to participants using extended 22 mm diameter breathing hoses passing through MSR conduits.
3. Provide standard-of-care patient monitoring as per ANZCA Guideline Document PS18. This includes end-tidal O₂, CO₂, N₂O measurement (where appropriate), pulse oximetry, 3-lead ECG, and non-invasive blood pressure measurement (NIBP).
 1. Monitor blood pressure as per ANZCA Guideline Document PS18 using a non-invasive blood pressure monitor located outside the MSR and connected by a long inflation tube to a cuff placed on the upper arm.
 2. Throughout the experiment, record and document all physiological parameters at 1 min intervals in addition to an automated recording of all parameters every 30 s.
4. Make sure that the gases are piped to participants using extended 22 mm diameter breathing hoses passing through MSR conduits. A suction system is located outside the MSR and a long delivery tube, connected to a Yankauer suction wand is passed through a conduit to be placed close to both the patient and clinical observer.
 1. In addition, ensure emesis basins are located close by within the MSR to enable their rapid positioning by the observer upon occurrence of emesis. The clinical observer within the MSR will need to remain vigilant to any airway obstruction, responding initially with a chin lift or jaw thrust and immediately discontinue the protocol if impending emesis is signaled by excessive swallowing or retching or airway obstruction is not resolved by the chin lift or jaw thrust.
5. Record EEG using an MEG compatible 64-channel Ag/AgCl electrode cap attached to a battery powered amplifier within the MSR. The amplifier is connected via a fiber-optic cable and a suitable media converter to a laptop running a compatible acquisition software.
6. Record brain magnetic field activity (MEG) at a sampling rate of 1000 Hz using an MEG system that has whole brain coverage and has well defined arrays of sensors that may include magnetometers and axial/planar gradiometers; the present study utilizing a system comprised of 102 magnetometers and 204 planar gradiometers. To avoid complexities not directly relevant to the protocol or the MEG system configuration, example data from the magnetometers alone is reported, although both magnetometer and gradiometer data is acquired as part of the protocol.
7. Track head position continuously using 5 head position indicator (HPI) coils. Digitize the location of the head coils, EEG electrodes and fiducial markers (nasion and left and right preauricular points) before MEG scanning using appropriate digitizing equipment.
 1. Because the aim is to obtain results in source space, disable any internal active shielding system employed by the MEG system for three-dimensional noise cancellations, in order to make the processing pipeline flexible with regards to the use of signal space separation (SSS) methods that are typically employed.
 2. Use an MRI scanner to obtain corresponding T1-weighted structural brain scans for later co-registration with M/EEG recordings.

3. Study Design and Protocol

NOTE: A two-way crossover experimental protocol is followed. Perform two separate testing sessions for each subject separated by a maximum of four weeks between testing sessions. One arm of the study consists of Xe administration while N₂O is given in the second arm. Participants

are blind to the type of gas being administered while the medical staff and researchers are not due to the slight differences in the procedure followed for their administration.

1. After informed consent is obtained, confirm participant eligibility with an extensive medical history interview and vital sign measurements which include blood pressure, heart rate, body temperature and peak expiratory flow. After participant eligibility is confirmed, the subject undergoes a brief measurement in the MEG to ensure that there are no unanticipated sources of noise.
2. Place the EEG cap on the subject's head and gel all electrodes. Attach the 5 HPI coils on the cap to continuously record head position in the MEG.
 1. Digitize the EEG-channels, HPI coil positions and extra points on the subject's nose and store all locations using the MEG's accompanying software package.
 2. Move the subject to the MSR, connect the electrode cap to the EEG amplifier and re-gel electrodes if required to ensure that their electrical contact impedances are below 5 k Ω .
3. In addition to the MEG and EEG, make three additional bipolar bio-channel recordings.
 1. Because anesthetic agent administration is associated with changes in muscle tone, record the electromyogram (EMG) using a pair of single-use Ag/AgCl electrodes placed submentally to record the activity of the mylohyoid and digastric (anterior belly) muscles.
 2. Record the electro-oculogram (EOG) by attaching a pair of electrodes above one of the eyes, near the brow, and near the corresponding lateral canthus and perform three-lead electrocardiogram (ECG) recordings using electrodes on each wrist and an elbow ground (see **Figure 1**).
4. Ask participants to keep the eyes closed during all recording phases of the experiment.
5. Perform clinical management of the subject with an anesthesiologist and an anesthetic nurse or other suitably trained clinical observer. Have the nurse/observer sit with the subject in the MSR in order to continuously monitor the participant's condition (in particular the face mask seal and subject's airway) and the anesthesiologist, located in the control room to manage gas delivery and electronic monitoring.
6. Collect data in a team of three: one member monitoring and controlling the acquisition of the MEG signal, another monitoring and controlling the acquisition of the EEG and another starting and stopping the computerized auditory continuous performance task while monitoring the subjects' responses, coordinating all experimental timings and recording minute blood pressure, and end-tidal gas concentrations and gas flow rate as provided by the anesthesiologist.
7. Continuously visually monitor the participant in the MSR via a suitable camera, which also records all stages of the experiment for subsequent assessment and review.
8. Behaviorally measure the ongoing level of responsiveness throughout the experiment using an auditory continuous performance task (aCPT). Use MEG compatible headphones to deliver a binaural auditory tone of either 1 or 3 kHz frequency of fixed stereo amplitude (approx. 76 dBA), with an inter-stimulus interval of between 2 to 4 seconds drawn from a uniform distribution.
 1. Ask the participant to respond as quickly as possible using two separate button boxes held in each hand. Use the left and right buttons on each box correspond to a low or high frequency tone, respectively, and the left and right button boxes, respectively, for the participant to indicate the absence or presence of nausea.
9. Closely monitor responsiveness throughout the experiment. The reaction time latency and accuracy (percentage of tones correctly classified) of the responses are automatically recorded as well as displayed on a monitor outside the MSR for the researchers to obtain a real time indication of the participants' behavioral state.
 1. Following multiple sequential right button box responses (indicating nausea), alert the observer in the MSR and the administering anesthesiologist that gas administration may need to be abruptly terminated to avoid emesis.
10. Record eyes closed resting EEG and MEG for 5 min followed by a 5 min eyes closed baseline EEG/MEG recording with the subject performing the aCPT task.
11. Remove the subject from the MSR and allow for a 20 gauge intravenous cannula to be placed in the left antecubital fossa by the anesthesiologist. Anti-emetic administration, occurring slowly over a period of 1 - 2 minutes, consisting of 4 mg dexamethasone and 4 mg ondansetron⁵⁹, follows to prevent any emesis caused by anesthetic gas inhalation, which is often observed with N₂O at the higher concentrations used⁶⁰.
12. Attach the face mask and breathing circuit to the subject using a modified sleep apnea continuous positive airways pressure (CPAP) harness, and assess for subject comfort and the absence of any leakage at 5 cm H₂O positive pressure.
13. Return the subject to the MSR to remain seated in the MEG for the remainder of the study.
14. Take a number of preventative steps to ensure limited subject movement during the simultaneous MEG and EEG recordings, since head and body movement can cause large artifacts in electromagnetic recordings and are expected to occur during the administration of the dissociative anesthetic agents due to their well-known propensity to induce psychomotor agitation.
 1. Place a custom-built cap made of a low density uncolored foam on the head which secures the head position inside the MEG dewar helmet irrespective of head size and shape.
 2. Further, use a cloth harness wrapped around the thighs and the gluteal muscles and secured to the back of the MEG chair to minimize any sagging/slouching that occurs in the participant's vertical position (see **Figure 1**).
 3. During the recording, track the head position continuously using the HPI coils, to view offline after completion of the experiment (see data analysis section for further details).
15. Once the participant is securely positioned, administer 100% inspired O₂ and continue this for up to 30 minutes until their end-tidal O₂ concentration is >90% indicating they are effectively de-nitrogenated, a process necessary to ensure accurate measurements of end-tidal anesthetic gas concentrations.
 1. During the last 5 minutes of denitrogenation, perform a final 5 minute eyes closed resting EEG/MEG aCPT recording to ensure that any effects anti-emetic administration and denitrogenation may have on brain activity can subsequently be determined and controlled for.
 2. Compare this third baseline recording to the previous baselines (rest eyes closed without anti-emetic and task eyes closed without anti-emetic) to determine the effects that antiemetic and aCPT have on spontaneous/resting M/EEG. The baselines are referred to

as baselines 1, 2 and 3 in the manuscript for rest eyes closed without anti-emetic, task eyes closed without anti-emetic and task eyes closed with anti-emetic, respectively.

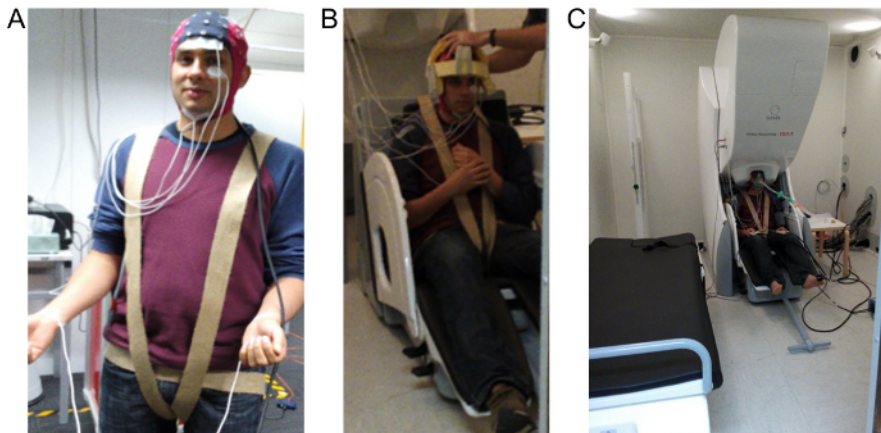


Figure 1: Images demonstrating EEG, EOG, EMG and ECG electrode layout and the overall set up within the MSR. (A) shows the 64-channel MEG compatible cap used to record the EEG, EOG is recorded using the two electrodes shown placed above and below the left eye, EMG is recorded using the two electrodes placed below the jaw and ECG is recorded using two electrodes placed on the wrist. (B) shows the custom-made foam cap and harness used to minimize subject movement during recording. (C) demonstrates the final configuration required for anesthetic administration which includes positioning the head within the MEG and attaching a tight fitting gas-mask. [Please click here to view a larger version of this figure.](#)

4. Gas Administration Protocol

NOTE: The gas administration protocol varies slightly depending on the arm of the study.

- Administer Xe at four step-wise increasing levels and N₂O at three step-wise increasing levels. The first three gas levels for each gas correspond to equi-MAC-awake levels of 0.25 (level 1), 0.5 (level 2) and 0.75 (level 3) times the MAC-awake concentration. These concentrations are 8%, 16%, 24% and 16%, 32%, 47% concentrations for Xe/O₂ and N₂O/O₂, respectively.
NOTE: The 4th level for Xe corresponds to 1.3 times the MAC-awake concentration.
- Choose the 4th gas level for Xe such that 95% of participants are expected to lose consciousness at this level (all subjects studied to date have achieved full loss of responsiveness during the aCPT task). Because of the well documented propensity of N₂O to induce nausea and vomiting at high concentrations, do not include a N₂O level at a concentration sufficient to induce loss of consciousness in 95% of participants (~75%). **Figure 2** summarizes the gas administration profiles.
- Follow the same experimental procedure for all equi-MAC Xe and N₂O levels with the exception of 42% Xe/O₂, which will require a slightly different methodology (see 4.4. below).
 - At the start of each level, inform the subject and anesthetic nurse/clinical observer that gas administration will commence and begin recording the EEG and MEG, signal to the administering anesthesiologist to begin gas administration and start the aCPT task. Gas wash-in then occurs for a period of 10 minutes such that the target end-tidal gas concentration is reached at the end of this period and maintained for 5 minutes (the assumed steady-state phase).
 - At the end of this 5 minute steady-state period, perform the wash-out with the administration of 100% O₂ over a period of 10 minutes during which end-tidal gas concentration returns to 0.
 - Repeat the procedure for the next step gas level.
NOTE: Loss of responsiveness (LOR) for Xe is expected to be achieved in 95% of participants at a concentration of 42% Xe/O₂⁶¹. The administration of this level occurs as for the lower levels until both the anesthetic nurse/clinical observer and the loss of button responses indicate LOR.
- Once LOR is achieved, maintain the Xe gas level for 10 minutes or until the anesthesiologist or anesthetic nurse/clinical observer consider it unsafe to continue after which wash-out with 100% O₂ takes places. Instances in which the anesthesiologist may consider it unsafe to continue include frequent pressing of the right button box indicating nausea, glottal noises, signs of emesis such as excessive salivation or swallowing and vaso-vagal reactions.
NOTE: At this highest level, exercise significant caution and set a low clinical threshold for discontinuing Xe gas administration. The authors' experience suggests that this level can be associated with a reduction in swallowing, the build-up of saliva and the appearance of retching-like behavior, that if allowed to continue may foreshadow regurgitation into the mask. Naturally, the consequences of this could include life threatening aspiration. It is also possible that less intense responses may occur at lower gas levels and thus exercise a high level of vigilance during the administration of *all* step-wise gas levels. In addition to these potential airway issues, be aware of the potential for vasovagal syncope, particularly in the younger male participants. Their age and the temporary fluid and food restrictions are all risk factors⁶².

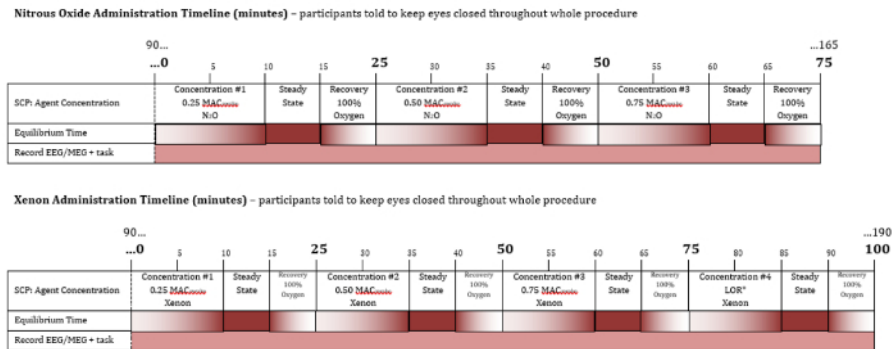


Figure 2: Summary of gas administration profiles for Xe and N₂O. Timeline and gas concentrations during the course of drug administration for N₂O (top) and Xe (bottom). The numbers above each timeline indicate the time in minutes since the start of the first gas delivery. Each level of peak equilibrated gas concentration is reached through a 10 minute equilibrating period, followed by a 5 minute steady state during which the peak equilibrated gas concentration is maintained, and then a 10 minute washout. The peak equilibrated gas concentrations increase sequentially over time. Note that the timeline of preparation for the experiment as well as the period after gas administration are not shown. [Please click here to view a larger version of this figure.](#)

5. Structural Scan

- Before the MRI, place vitamin E capsules on the participant's head to be used as markers to highlight the digitized fiducial points for the nasal apex and left and right preauricular points. This ensures a better co-registration of the MEG/EEG sensors and MRI brain scans when attempting to relate MEG/EEG source imaging to MRI-based neuroanatomy.
- Obtain a single structural T1-weighted MRI scan, either *after* the completion of an arm of the study if the participant is feeling well, otherwise ask them to return on a separate day for the structural brain scan.

6. Participant Follow-up

NOTE: The subject is free to leave when accompanied by a friend or relative.

- Upon discharge, ask the participant to complete a truncated version of the 5-Dimensional Altered States of Consciousness Rating Scale (5D-ASC); a questionnaire designed to access individual differences by comparing normal and altered consciousness status by means of a visual analogue scale^{63,64}.
- In addition, ask for the submission of a short narrative of their overall experience during the experiment as well as specific details about level dependent qualitative effects.
- Have both of these documents completed and sent to the researchers 24 hours after each recording session.

7. Data Analysis

NOTE: This section describes basic data analysis at the MEG/EEG sensor level covering the steps involved in generating examples of preprocessed MEG/EEG data, spectral topography, head movements, responsiveness scoring, and auditory evoked responses. The focus of this article is on the illustration of typical examples so that the reader can understand the important features of the recorded data. No intra-individual or group-wise statistical analyses are performed as the principle aim in this analysis section is to detail important pre-processing steps that attest to the quality and integrity of the data collected. No details are provided for the myriad analyses that could be performed on this data^{55,56} as they fall outside the scope of the description of the method.

- Complete offline data analysis on a desktop computer using appropriate data analysis software and use relevant toolboxes for both EEG and MEG data processing. In the authors' pipeline, use version 20160801 of the Fieldtrip toolbox⁶⁵.
- Compute head movement during each MEG recording by first obtaining the continuous head positions as a sequence of quaternion co-ordinates by analyzing the 5 HPI coil signals saved as part of each of the level dependent and baseline MEG recordings. Convert head positions from quaternion into Cartesian co-ordinates.
- Assemble the 6 and 7 recordings for N₂O and Xe study arms (baselines 1, 2 and 3, gas levels 1 to 3 or 1 to 4 respectively). Time shift raw EEG relative to MEG data in order to synchronize the two signal types based on a common trigger channel. This form of synchronization arises from the choice of EEG recording system.
NOTE: Many MEG systems contain a built in EEG system that offers very accurate electronic level synchronization of the MEG & EEG, but often have low resolution DAC quantization of 16 bits. For this reason, utilize an external EEG system (see 2.3) having higher 24-bit EEG amplitude resolution to enable a higher tolerance to electrode offset potentials, the measurement of low frequency information and a flat frequency response across all channels.
- For all recordings involving gas delivery and aCPT performance, redefine time zero to the commencement of aCPT task/gas delivery.
- Visually inspect raw MEG data and exclude any bad channels from further analysis. Next, filter the data using a temporal signal-space separation algorithm⁷⁶ implemented in the MEG-system software. The algorithm suppresses sources of magnetic interference outside the sensor array and hence results in a reduction of external or rigid body movement artifacts. Import the output data set into the data analysis software to be used with the magnetometers (102 channels) selected for further processing.
- Band-pass filter the MEG at 2 to 50 Hz and apply line noise filters at 50, 100 and 150 Hz. Visual artifact detection and an automatic artifact detection procedure implemented in the Fieldtrip software allow for the removal of any artifactual elements. Visually inspect any segments

containing eye blinks, heart beats or muscular artifacts and exclude from the data, as well as any segments correlated with significant changes in head movement greater than 5 mm (see below).

NOTE: Movements of greater than 5 mm with respect to the beginning of each 5 minute baseline or gas equilibrated period are used to reject continuously acquired MEG data since MEG source imaging typically has a spatial resolution of the order of 5 mm (e.g. for MEG/EEG beamformers⁵⁵). It is however possible to perform movement compensation of the MEG data⁶⁶ rather than rejecting data segments correlated with significant head movement, however such methods are beyond the scope of this paper.

7. As with MEG data, visually inspect the 64-channel raw EEG and exclude any bad channels from further data analysis. Band-pass filter the data using the same frequency ranges as for the MEG. Re-reference the EEG to a common average as is standard for source imaging approaches. Finally, remove any segments containing artifacts contemporaneous with those of the corresponding MEG.
8. To visualize the spectral properties of the MEG/EEG data, compute single-sided amplitude spectra along the anterior-posterior midline for the EEG channels FPz, Cz and Oz and for midline frontal, central and occipital MEG magnetometer channels (**Figure 3**).
 1. Calculate the sensor-level topographic map of alpha band (8-13 Hz) power for MEG/EEG, given that strong alpha band changes have been observed previously for N₂O and GABAergic anesthetics^{25,31,67}.
 2. For EEG data, use the FPz channel as the reference to calculate the topographic alpha band power in order to better highlight alpha power changes.

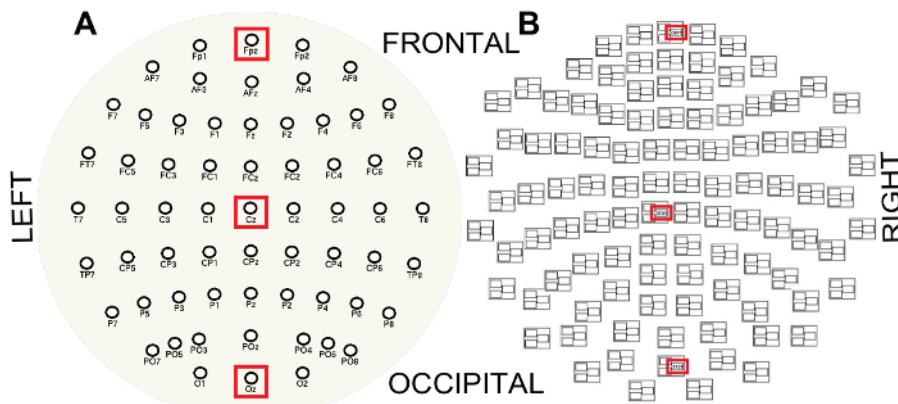


Figure 3: EEG (A) and MEG (B) sensor layouts viewed from the top of the head and flattened into a plane. Note the MEG triplet structure where sensors ending in ###1 are magnetometers and sensors ending in ###2 or ###3 are gradiometers. Red boxes indicate the channels along the anterior-posterior midline used to visualize the spectral properties of the EEG and MEG, FPz (frontal), Cz (central) and Oz (occipital) and frontal, central and occipital magnetometer channels respectively. [Please click here to view a larger version of this figure.](#)

9. Obtain auditory evoked responses for filtered artifact-free MEG and EEG data for each recording involving the aCPT task. Epoch the signals from -1000 ms to +2000 ms relative to the tone trigger times and average all available artifact free epochs. Take the latency between stimulus trigger generation and delivery of sound to the ear into account, in this case 190.5 ms.

Representative Results

This section utilizes data obtained from one subject in order to demonstrate the typical features of the simultaneous recordings and the potential of such information to contribute a better understanding of anesthetic induced altered states of consciousness. To simplify the exposition, results are shown for i) recordings of the post-anti-emetic administration baseline (baseline 3), ii) 0.75 equi-MAC-awake peak gas concentrations (level 3) of N₂O (47%) and Xe (24%), and iii) Xe peak gas concentration of 42% (level 4). Levels 3 and 4 were chosen as they are the highest steady-state levels considered for N₂O and Xe, respectively. Moreover, level 4 Xe involves a clear loss of responsiveness, a state not typically achievable for N₂O.

In order to clearly illustrate the extent of head movement the absolute positions of all 5 HPI coils are shown as a function of time during multiple recordings. **Figure 4** clearly demonstrates that the steps followed to ensure limited movement during the scans are associated with acceptable levels of head and body movement despite pharmacological intervention. A notable example of extensive head movement can be seen in **Figure 4(ii)** between 20-25 minutes (during the washout period) when large head movement was recorded. Such periods are visually detected and removed from the data. The protocol ensures that stable end-tidal gas concentrations at all levels can be easily and readily achieved (see **Figure 4**), with subject responsiveness robustly assessed using the aCPT task. **Figures 4(ii) and 4(iv)** clearly show such assessed reductions in responsiveness during the 5 minute steady state phases for both xenon and nitrous oxide. **Figure 4(v)** indicates loss of responsiveness (0% accuracy) during the steady state period under 42% Xe administration, as expected.

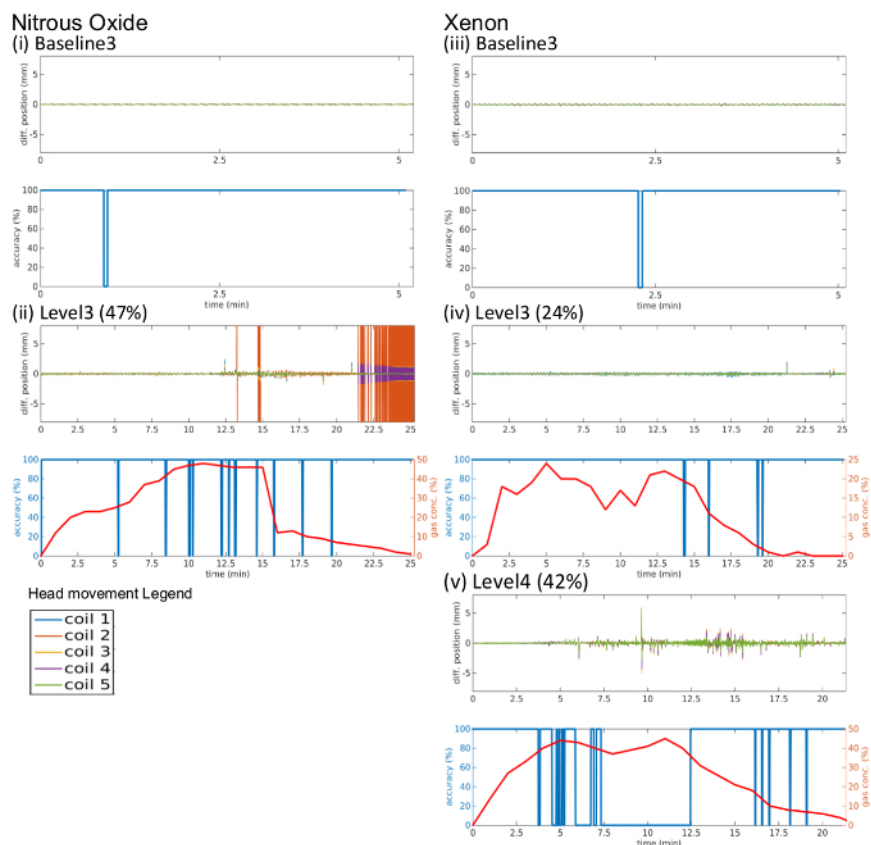


Figure 4: Examples of head movement, gas concentration and aCPT accuracy time series from one participant for (i) baseline 3 (post antiemetic) prior to N₂O administration, (ii) 47% N₂O (level 3), (iii) baseline 3 prior to Xe administration, (iv) 24% Xe (level 3), and (v) 42% Xe (level 4). Each sub-figure shows absolute movement (top) of the 5 head coils (legend below (ii) indicates coils) and gas concentration (bottom, red) and aCPT accuracy (bottom, blue) as a function of time in minutes. [Please click here to view a larger version of this figure.](#)

Examples of the filtered artifact-free MEG and EEG data along the anterior-posterior mid-line for the same subject as in figure 4 are shown for time aligned 10 second segments for N₂O and Xe in **Figure 5**. Baseline 3 (post antiemetic) for both Xe and N₂O shows strong alpha oscillations in the occipital channels (Oz for EEG and an occipital magnetometer channel for MEG). As the anesthetic level increases for level 3 N₂O (47% peak gas) total signal power is reduced, with reductions in alpha band power particularly evident. In contrast alpha activity, in response to Xe administration is not significantly reduced until level 4 (42% peak gas). In contrast to N₂O increasing Xe concentrations are more clearly associated with an increase in the amplitude of delta (0 - 4 Hz) and theta (4 - 8 Hz) band activity, being especially clear in the central site during 42% administration (level 4) in the MEG.

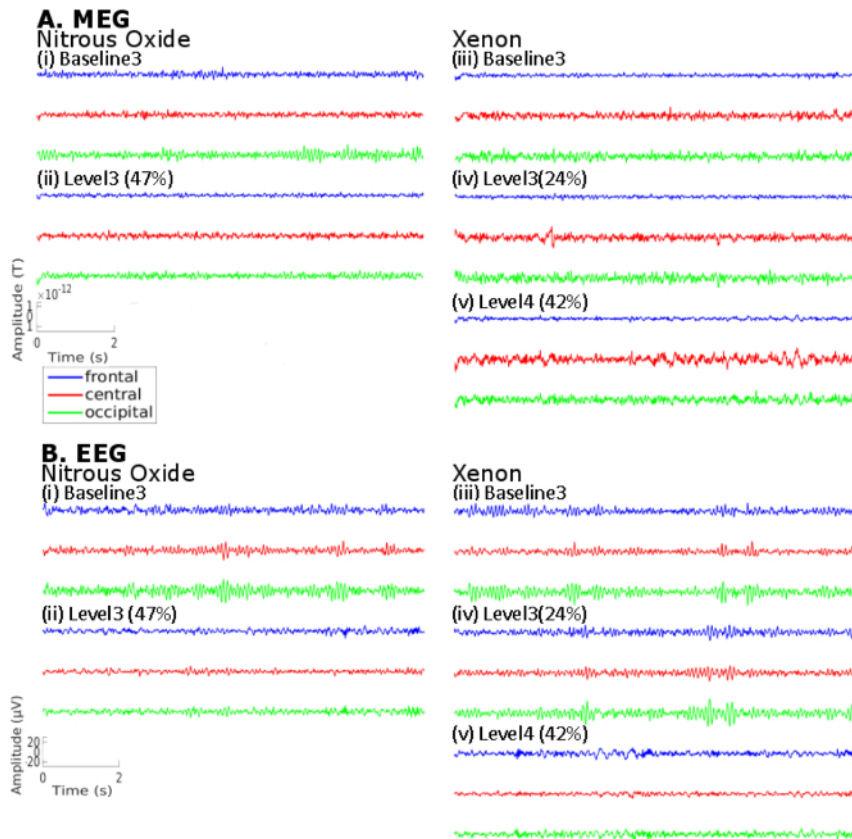


Figure 5: Example of a time aligned 10 second window of filtered artifact-free (A) MEG and (B) EEG data for the same subject in Figure 4 for the cases of (i) baseline 3 (post antiemetic) prior to N₂O administration, (ii) 47% N₂O (level 3), (iii) baseline 3 (post antiemetic) prior to Xe administration, (iv) 24% Xe (level 3), (v) 42% Xe (level 4). For 24% Xe and 47% N₂O, the time period selected was a fragment of the 5 minute steady state while for 42% Xe, the epoch of data selected was during the period of loss of responsiveness, as indicated by the subject's aCPT response. Frontal (blue), central (red) and occipital (green) correspond to the respective MEG magnetometer and EEG channels. [Please click here to view a larger version of this figure.](#)

The changes in signal power observed in **Figure 5** are further detailed in single-sided amplitude spectra of the same signals in **Figure 6**. While there emerge a range of observed changes in power when transitioning from baseline to gas, the most significant changes appear to be the gradual attenuation of the strong baseline alpha band (8-13 Hz) power, observed in the occipital electrodes, with increasing gas concentrations. This is complemented with increasing low frequency delta and theta band activity.

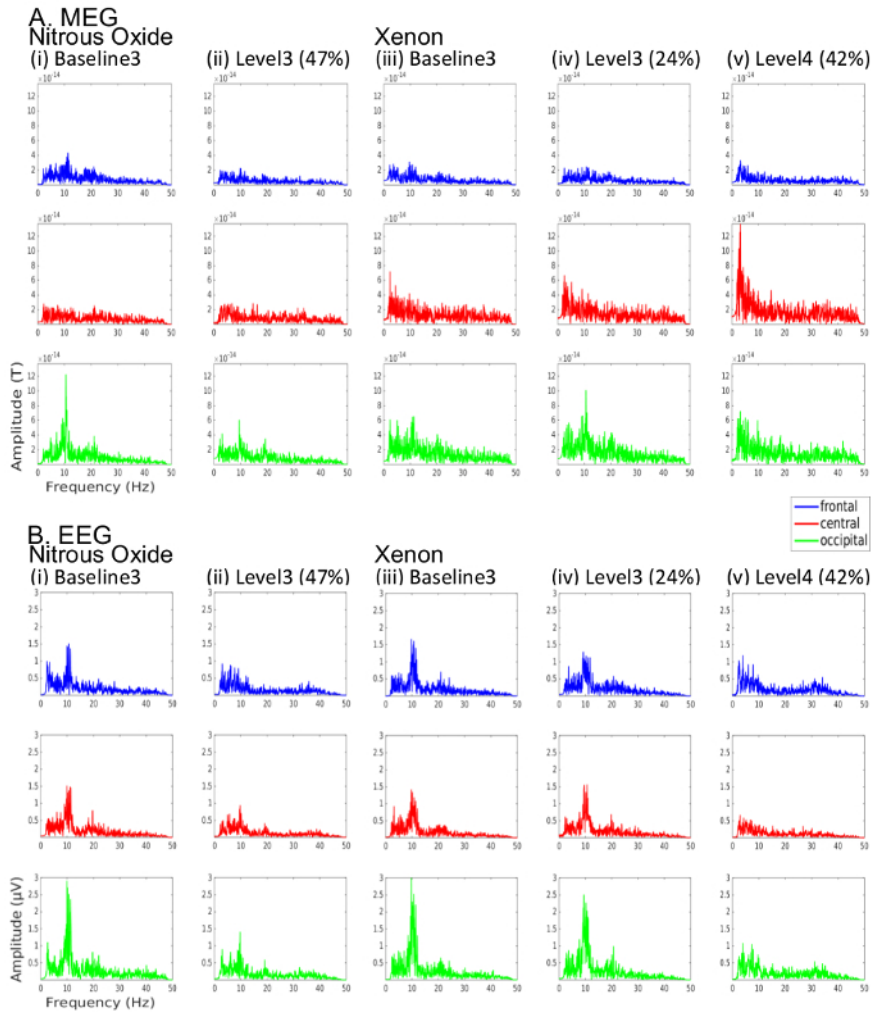


Figure 6: Amplitude spectra for the same (A) MEG and (B) EEG data shown in Figure 5 for the cases of (i) baseline 3 (post antiemetic) prior to N_2O administration, (ii) 47% N_2O (level 3), (iii) baseline 3 (post antiemetic) prior to Xe administration, (iv) 24% Xe (level 3), (v) 42% Xe (level 4). Frontal (blue), central (red) and occipital (green) channels correspond to respective MEG magnetometer and EEG channels. [Please click here to view a larger version of this figure.](#)

Figure 7 illustrates an example of the topographic changes in alpha band power linked to increases in Xe and N_2O gas concentration. Note the clear attenuation of posterior alpha power with increases in Xe and N_2O , consistent with changes observed previously for N_2O and GABAergic anesthetics^{25,31,67}.

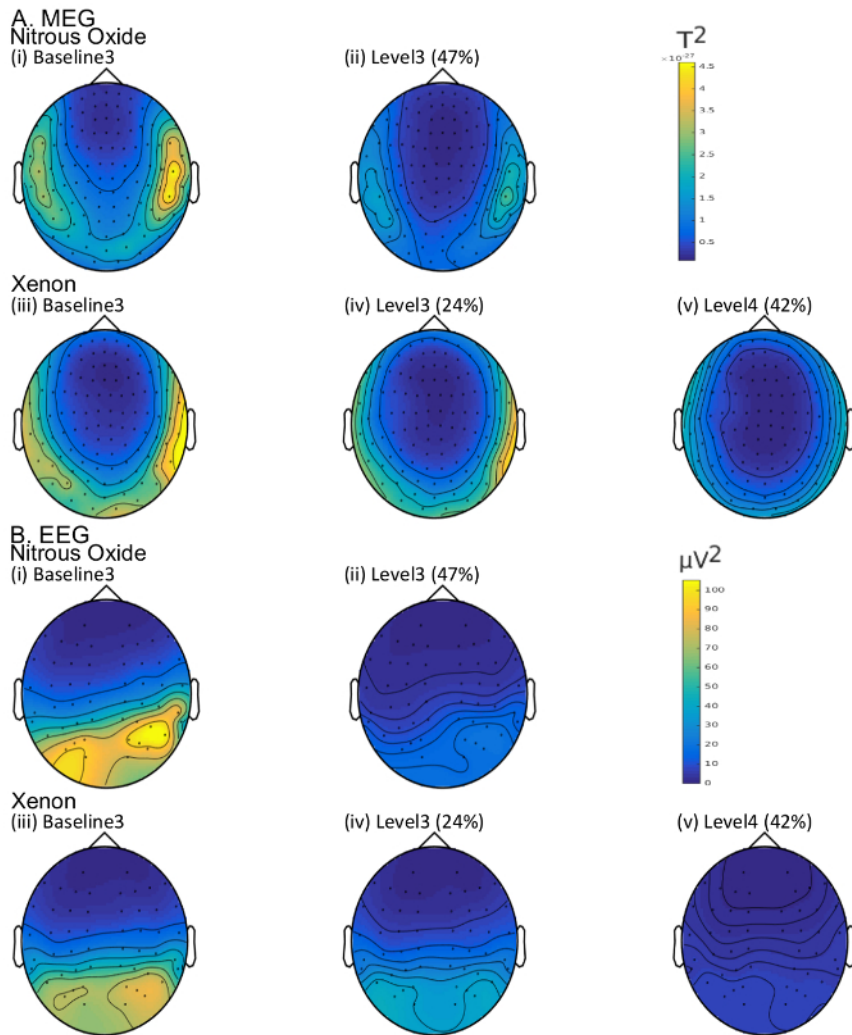


Figure 7: Topographic alpha (8-13 Hz) band power in the (A) MEG (magnetometers only) and (B) EEG for the same subject as in Figures 5 and 6 for the cases of (i) baseline 3 (post antiemetic) prior to N₂O administration, (ii) 47% N₂O (level 3), (iii) baseline 3 (post antiemetic) prior to Xe administration, (iv) 24% Xe (level 3), (v) 42% Xe (level 4). [Please click here to view a larger version of this figure.](#)

Finally, **Figure 8** illustrates example sensor-level MEG and EEG auditory evoked responses obtained with the protocol and aCPT task for the same subject as in **Figures 5-7**. It can be noted that increases in in Xe and N₂O gas concentration lead to a weakening of the first response peak and also to the delay, attenuation or disappearance of later response peaks, especially during loss of responsiveness for Xe level 4 (42%).

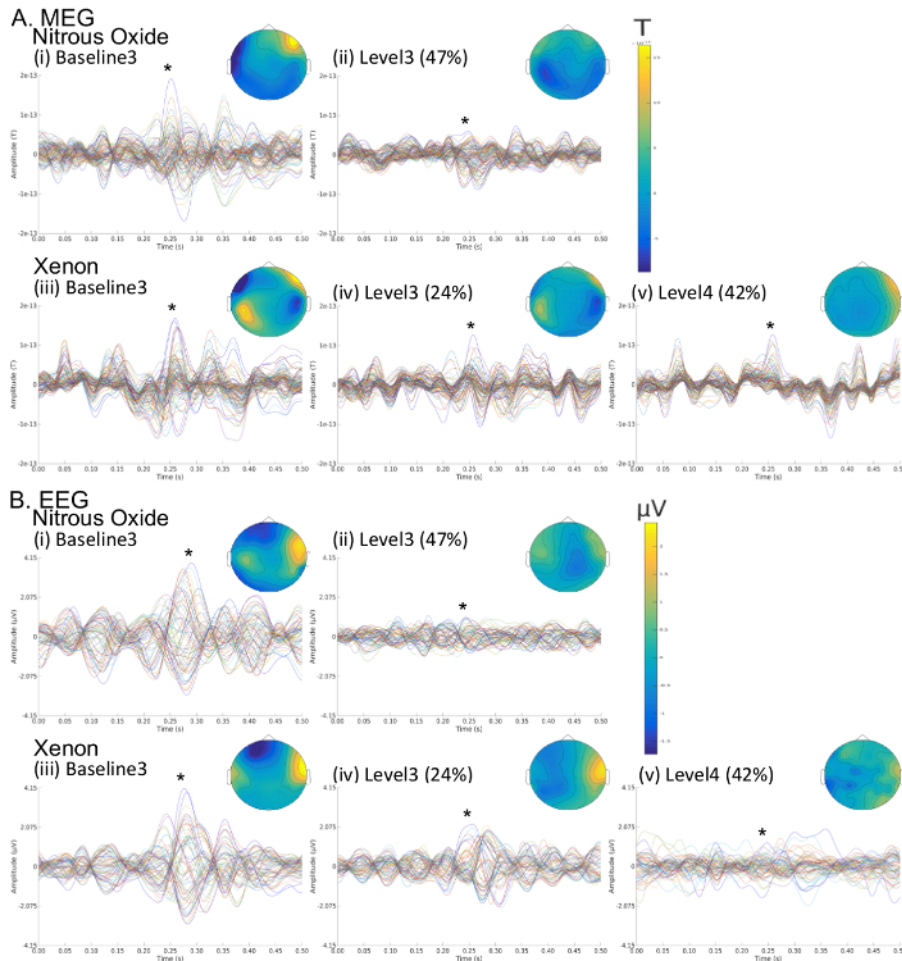


Figure 8: Sensor-level auditory evoked responses for the (A) MEG and (B) EEG for the same subject as in Figures 5-7 for the cases of (i) baseline 3 (post antiemetic) prior to N₂O administration, (ii) 47% N₂O (level 3), (iii) baseline 3 (post antiemetic) prior to Xe administration, (iv) 24% Xe (level 3), (v) 42% Xe (level 4). Colored butterfly plots correspond to channel-wise time ensemble responses. For each butterfly plot the topographic map corresponds to the time of peak response. [Please click here to view a larger version of this figure.](#)

Discussion

This paper has outlined a comprehensive protocol for the simultaneous recording of MEG and EEG during anesthetic gas delivery with N₂O and Xe. Such a protocol will be valuable for studying the electromagnetic neural correlates of anesthetic-induced reductions in consciousness. The protocol is also expected to generalize to the delivery of other anesthetic gases such as sevoflurane or isoflurane. This will facilitate a greater understanding of the common, specific and distinct macroscopic mechanisms that underlie anesthetic-induced reductions in consciousness for a range of anesthetics having quite different molecular modes and targets of action. Understanding how anesthetics function is arguably one of the great outstanding problems of neuroscience and is arguably key to understanding the neurochemical basis of behavior.

The example results presented are entirely consistent with previous studies investigating anesthetic induced EEG power spectral changes, thus attesting to the fidelity of the protocol we have developed and outlined. In the case of N₂O administration, the results summarized above are in line with decreases in delta, theta and alpha band power in the EEG that have been observed for high inspired levels of N₂O (>40%)^{25,28,31}. Similarly, during Xe anesthesia our results are consistent with the few published reports on the effects of Xe using high density EEG. For example, Johnson *et al.*²⁹ demonstrated a slowing of the EEG with increased total power in the delta and theta bands especially in frontal regions, results that accord well with the typical results we have presented here. Further Johnson *et al.* identified that Xe inhalation was associated with increases in both frontal and posterior midline delta, with these slow wave activity changes being topographically inhomogeneous in nature, an observation that mirrors the variability in frequency band topography along the anterior-posterior axis demonstrated in this investigation's results. In reference to changes in higher frequency activity (alpha band and above), the picture becomes much less clear. Hartmann *et al.*³⁴ described a decrease in global alpha activity, somewhat resembling the authors' results, and a global increase in beta band (13 - 30 Hz) power, whereas Laitio *et al.*³³ showed an increase in frontal alpha and a decrease in posterior alpha activity. In the beta and gamma frequency ranges Johnson *et al.*²⁹ reported widespread increases in gamma band (35 - 45 Hz) power whereas Goto *et al.*³² showed a decrease. In summary, this method is well able to elicit changes in electromagnetic brain activity that have been reported for N₂O and Xe using much simpler recording configurations.

We have shown clear examples of the effects that the gaseous anesthetic agents Xe and N₂O induce in the, amplitude spectra, alpha band power topography and auditory evoked responses of filtered artefact-free MEG/EEG data. More elaborate data analysis methods can be

expected to offer important insight into the mechanisms of anesthetic action and the corresponding global and local alterations in network connectivity that occur in states of altered consciousness. Moving beyond the sensor-level data and looking at source activity will provide a representation of the changes in spontaneous activity that can be better related to neuroanatomy (for a review see ⁵⁵). Applying various functional connectivity measures (for a review see ⁵⁶) to this source-level data will be expected to contribute to further understanding the role that disruptions in functional connectivity have in anesthetic-induced reductions in consciousness¹.

To date pharmaco-MEG has been under-utilized for the characterization of anesthetic action, with the exception of a hand full of studies on diagnostic sedation or enhancement of epileptogenic activity in epilepsy patients. Notable examples of such MEG studies include Hall *et al.*^{68,69} where a single oral dose of diazepam was administered, Cornwell *et al.*⁷⁰ where sub-anesthetic ketamine was infused, Saxena *et al.*⁷¹ which looked at propofol sedation, and Quaedflieg *et al.*⁷²'s investigations of the effects of remifentanyl on mismatch negativity. More recently, Muthukumaraswamy and colleagues⁷³ employed the MEG in a functional connectivity investigation of sedative doses of ketamine revealing important oscillatory changes, notably in alpha, theta and gamma power, as well as significant alterations in NMDA-mediated frontal-to-parietal connectivity. Our results clearly demonstrate the potential and utility of simultaneously recorded MEG and high-density EEG in exploring the mechanisms of anesthesia. To the authors' knowledge no prior simultaneous MEG/EEG study has been performed in humans with volatile or gaseous anesthetic agents and thus the method outlined here will hopefully stimulate further efforts in this direction.

There are several limitations associated with our protocol that should be mentioned. Firstly, the experimental procedure was designed with gaseous anesthetic administration in mind and important, and as yet untried, modifications will need to be considered when using other types of anesthetics such as the volatile agents best exemplified by sevoflurane. In the case of volatile inhalation anesthetics, we recommend the use of a laryngeal mask airway to ensure airway patency, however the invasive nature of the procedure should be noted. Secondly, we chose a very simple auditory continuous performance task to monitor responsiveness. A simple auditory continuous performance paradigm was selected since event related changes were not the primary focus of this investigation. For investigating more detailed correlations between brain activity and cognition during anesthesia more complex and salient auditory⁷⁷, visual⁷¹ and tactile⁷⁸ stimuli will need to be utilized. Head movement during anesthesia is also a possible imaging confound which we have addressed through the use of a custom-built foam cap which keeps the head secure in the MEG dewar, a harness that keeps the participant secure in the MEG chair, and strict data artifact removal procedures. Finally, an explicit human factors analysis⁷⁹ that could quantify the extent to which other investigators could easily follow this protocol is missing from this paper. While we did provide several notes on the limitations and other factors associated with performing inhalation anesthesia using xenon and N₂O while recording EEG/MEG, the development of specific metrics of performance could have been utilized in order to indicate the relative deployment of resources and time to specific sections of the protocol.

The findings outlined in here clearly demonstrate that it is possible to simultaneously record MEG and EEG in the restrictive setting of the MEG magnetically shielded environment while ensuring high quality data that is associated with minimal head movement and adventitious artifact. Such methods are likely to have significant clinical implications as they can be utilized to better understand any possible universal mechanisms of anesthesia, which in turn could lead to improvements in clinical monitoring of anesthetics by preventing incidents of perioperative awareness and improving post-operative outcomes^{74,75}. Moreover, the setup is not necessarily limited to anesthesia investigations but can be modified accordingly to accommodate various types of pharmacological interventions, gaseous or otherwise.

Disclosures

The authors have nothing to disclose.

Acknowledgements

The authors would like to thank Mahla Cameron Bradley, Rachel Anne Batty and Johanna Stephens for valuable technical assistance with MEG data collection. Thanks are additionally extended to Dr. Steven McGuigan for support as a second anesthesiologist. Paige Pappas provided invaluable anesthetic nurse oversight. Markus Stone graciously proffered his time and expertise in editing and filming the protocol. Dr. Suresh Muthukumaraswamy gave specific advice regarding data analysis and the interpretation of results. Finally, Jarrod Gott contributed many a stimulating discussion, helped in the execution of a number of pilot experiments and was central in the design of the foam head brace.

This research was supported by a James S. McDonnell collaborative grant #220020419 "Reconstructing Consciousness" awarded to George Mashour, Michael Avidan, Max Kelz and David Liley.

References

1. Hudetz, A. Suppressing the Mind. *Hudetz A, Pearce R, editors, Suppressing the Mind*. 178-189 (2010).
2. Franks, N. P., Dickinson, R., de Sousa, S. L., Hall, A. C., & Lieb, W. R. How does xenon produce anaesthesia? *Nature*. **396** (6709), 324 (1998).
3. Jevtović-Todorović, V., Todorović, S.M., Mennerick, S., Powell, S., Dikranian, K., Benshoff, N., Zorumski, C.F., Olney, J.W. Nitrous oxide (laughing gas) is an NMDA antagonist, neuroprotectant and neurotoxin. *Nat Med*. **4** (4), 460-463 (1998).
4. Alkire, M. T., Hudetz, A. G., & Tononi, G. Consciousness and Anesthesia NIH Public Access. **322** (5903), 876-880 (2009).
5. Fiset, P., *et al.* Brain Mechanisms of Propofol-Induced Loss of Consciousness in Humans: a Positron Emission Tomographic Study. *The J Neurosci*. **19** (13), 5506-5513 (1999).
6. Schlünzen, L., *et al.* Effects of subanaesthetic and anaesthetic doses of sevoflurane on regional cerebral blood flow in healthy volunteers. A positron emission tomographic study. *Acta Anaesthesiologica Scandinavica*. **48** (10), 1268-1276 (2004).
7. Alkire, M. T., *et al.* Cerebral Metabolism during Propofol Anesthesia in Humans Studied with Positron Emission Tomography. *Anesthesiology*. **82**, 393-403 (1995).
8. Alkire, M. T., Haier, R. J., Shah, N. K., Anderson, C. T. Positron Emission Tomography Study of Regional Cerebral Metabolism in Humans during Isoflurane Anesthesia. *Anesthesiology*. **86**, 549-57 (1997).

9. Alkire, M. T., *et al.* Functional Brain Imaging during Anesthesia in Humans. Effects of Halothane on Global and Regional Cerebral Glucose Metabolism. *Anesthesiology*. **90**, 701-709 (1999).
10. Kaike, K.K., *et al.* Effects of surgical levels of propofol and sevoflurane anesthesia on cerebral blood flow in healthy subjects studied with positron emission tomography. *Anesthesiology*. **6**, 1358-1370 (2002).
11. Prielipp, R. C., *et al.* Dexmedetomidine-induced sedation in volunteers decreases regional and global cerebral blood flow. *Anesthesia and analgesia*. **95** (4), 1052-1059, table of contents (2002).
12. Mukamel, E. A., *et al.* A transition in brain state during propofol-induced unconsciousness. *J Neurosci*. **34** (3), 839-45 (2014).
13. Boveroux, P., Vanhaudenhuyse, A., & Phillips, C. Breakdown of within- and between-network Resting State during Propofol-induced Loss of Consciousness. *Anesthesiology*. **113** (5), 1038-1053 (2010).
14. Pelligrino, D.A., Miletich, D.J., Hoffman, W.E., Albrecht, R.F. Nitrous oxide markedly increases cerebral cortical metabolic rate and blood flow in the goat. *Anesthesiology*. **60** (5), 405-412 (1984).
15. Hansen, T. D., Warner, D. S., Todd, M. M., & Vust, L. J. The role of cerebral metabolism in determining the local cerebral blood flow effects of volatile anesthetics: evidence for persistent flow-metabolism coupling. *J Cereb Blood Flow Metab*. **9**, 323-328 (1989).
16. Roald, O. K., Forsman, M., Heier, M. S., & Steen, P. A. Cerebral effects of nitrous oxide when added to low and high concentrations of isoflurane in the dog. *Anesth Analg*. **72** (1), 75-79 (1991).
17. Algotsson, L., Messeter, K., Rosén, I., Holmin, T. Effects of nitrous oxide on cerebral haemodynamics and metabolism during isoflurane anaesthesia in man. *Acta Anaesthesiol Scand*. **36** (1), 46-52 (1992).
18. Field, L.M., Dorrance, D.E., Krzeminska, E.K., Barsoum, L.Z. Effect of nitrous oxide on cerebral blood flow in normal humans. *Br J Anaesth*. **70** (2), 154-9 (1993).
19. Matta, B.F., Lam, A.M. Nitrous oxide increases cerebral blood flow velocity during pharmacologically induced EEG silence in humans. *J Neurosurg Anesthesiol*. **7** (2), 89-93 (1995).
20. Langsjo, J. W., *et al.* Effects of subanesthetic doses of ketamine on regional cerebral blood flow, oxygen consumption, and blood volume in humans. *Anesthesiology*. **99** (3), 614-623 (2003).
21. Reinstrup, P., *et al.* Regional cerebral metabolic rate (positron emission tomography) during inhalation of nitrous oxide 50% in humans. *Br J Anaesth*. **100** (1), 66-71 (2008).
22. Rex, S., *et al.* Positron emission tomography study of regional cerebral blood flow and flow-metabolism coupling during general anaesthesia with xenon in humans. *Br J Anaesth*. **100** (5), 667-675 (2008).
23. Laitio, R. M., *et al.* Effects of xenon anesthesia on cerebral blood flow in humans. *Anesthesiology*. **106** (6), 1128-1133 (2007).
24. Laitio, R. M., *et al.* The effects of xenon anesthesia on the relationship between cerebral glucose metabolism and blood flow in healthy subjects: A positron emission tomography study. *Anesthesia and Analgesia*. **108** (2), 593-600 (2009).
25. Yamamura, T., Fukuda, M., Takeya, H., Goto, Y., & Furukawa, K. Fast oscillatory EEG activity induced by analgesic concentrations of nitrous oxide in man. *Anesth Analg*. **60** (5), 283-288 (1981).
26. Rampil, I.J., Kim, J.S., Lenhardt, R., Negishi, C., S. DI Bispectral EEG index during nitrous oxide administration. *Anesthesiology*. **89** (3), 671-677 (1998).
27. Maksimow, A., *et al.* Increase in high frequency EEG activity explains the poor performance of EEG spectral entropy monitor during S-ketamine anesthesia. *Clinical Neurophysiology*. **117** (8), 1660-1668 (2006).
28. Foster, B. L., & Liley, D. T. J. Effects of nitrous oxide sedation on resting electroencephalogram topography. *Clinical Neurophysiology*. **124** (2), 417-423 (2013).
29. Johnson, B. W., Sleight, J. W., Kirk, I. J., & Williams, M. L. High-density EEG mapping during general anaesthesia with Xenon and propofol: A pilot study. *Anaesthesia and Intensive Care*. **31** (2), 155-163 (2003).
30. Foster, B. L., Bojak, I., & Liley, D. T. J. Population based models of cortical drug response: Insights from anaesthesia. *Cognitive Neurodynamics*. **2** (4), 283-296 (2008).
31. Kuhlmann, L., & Liley, D. T. J. Assessing nitrous oxide effect using electroencephalographically-based depth of anesthesia measures cortical state and cortical input. *J Clin Monit Comput*. (2017).
32. Goto, T., *et al.* Bispectral analysis of the electroencephalogram does not predict responsiveness to verbal command in patients emerging from xenon anaesthesia. *Br J Anaesth*. **85** (3), 359-363 (2000).
33. Laitio, R. M., Kaskinoro, K., Maksimow, A., Kangas, K., & Scheinin, H. Electroencephalogram during Single-agent Xenon. *Anesthesiology*. **18** (1), 63-70 (2008).
34. Hartmann, A., Dettmers, C., Schuier, F. J., Wassmann, H. D., & Schumacher, H. W. Effect of stable xenon on regional cerebral blood flow and the electroencephalogram in normal volunteers. *Stroke*. **22** (2), 182-189 (1991).
35. Lee, U., Müller, M., Noh, G.-J., Choi, B., & Mashour, G. a Dissociable network properties of anesthetic state transitions. *Anesthesiology*. **114** (4), 872-881 (2011).
36. Ku, S. W., Lee, U., Noh, G. J., Jun, I. G., & Mashour, G. A. Preferential inhibition of frontal-to-parietal feedback connectivity is a neurophysiologic correlate of general anesthesia in surgical patients. *PLoS ONE*. **6** (10), 1-9 (2011).
37. Kuhlmann, L., Foster, B. L., & Liley, D. T. J. Modulation of Functional EEG Networks by the NMDA Antagonist Nitrous Oxide. *PLoS ONE*. **8** (2) (2013).
38. Greicius, M. D., *et al.* Persistent default-mode network connectivity during light sedation. *Human Brain Mapping*. **29** (7), 839-847 (2008).
39. Deshpande, G., Sathian, K., & Hu, X. Assessing and compensating for zero-lag correlation effects in time-lagged granger causality analysis of fMRI. *IEEE Transactions on Biomedical Engineering*. **57** (6), 1446-1456 (2010).
40. Schrouff, J., *et al.* Brain functional integration decreases during propofol-induced loss of consciousness. *NeuroImage*. **57** (1), 198-205 (2011).
41. Langsjo, J. W., *et al.* Returning from Oblivion: Imaging the Neural Core of Consciousness. *J Neurosci*. **32** (14), 4935-4943 (2012).
42. Mukamel, E. A., Wong, K. F., Prerau, M. J., Brown, E. N., & Purdon, P. L. Phase-based measures of cross-frequency coupling in brain electrical dynamics under general anesthesia. *Conf Proc IEEE Eng Med Biol Soc, EMBS*. **6454**, 1981-1984 (2011).
43. Logothetis, N. K. What we can do and what we cannot do with fMRI. *Nature Reviews Neuroscience*. **453** (June), 869-878 (2008).
44. Nunez, P.L., Srinivasan, R. *Electric fields of the brain: the neurophysics of EEG*. Oxford University Press, USA: (2006).
45. Härmäläinen, M. S., Hari, R., Ilmoniemi, R. J., Knuutila, J., & Lounasmaa, O. V Magnetoencephalography - theory, instrumentation, and applications to noninvasive studies of the working human brain. *Rev Modern Physics*. **65** (2), 413-505 (1993).
46. Nunez, P. L., & Srinivasan, R. A theoretical basis for standing and traveling brain waves measured with human EEG with implications for an integrated consciousness. *Clinical Neurophysiology*. **117** (11), 2424-2435 (2006).

47. Kayser, J., & Tenke, C. E. In search of the Rosetta Stone for scalp EEG: Converging on reference-free techniques. *Clinical Neurophysiology*. **121** (12), 1973-1975 (2010).
48. Barkley, G.L., Baumgartner, C. MEG and EEG in epilepsy. *J Clin Neurophysiol*. **20** (3), 163-78 (2003).
49. Parra, L. C., & Bikson, M. Model of the effect of extracellular fields on spike time coherence. *Conference proceedings: ... Annual International Conference of the IEEE Engineering in Medicine and Biology Society. IEEE Engineering in Medicine and Biology Society. Annual Conference*. **6**, 4584-7 (2004).
50. Liu, A. K., Dale, A. M., & Belliveau, J. W. Monte Carlo simulation studies of EEG and MEG localization accuracy. *Human Brain Mapping*. **16** (1), 47-62 (2002).
51. Cullen, S.C., Eger, E.I. 2nd, Cullen, B.F., Gregory, P. Observations on the anesthetic effect of the combination of xenon and halothane. *Anesthesiology*. **31** (4), 305-9 (1969).
52. Hornbein, T. F., et al. The minimum alveolar concentration of nitrous oxide in man. *Anesth Analg*. **61** (7), 553-556 (1982).
53. Fahlenkamp, A. V., et al. Evaluation of bispectral index and auditory evoked potentials for hypnotic depth monitoring during balanced xenon anaesthesia compared with sevoflurane. *Br J Anaesth*. **105** (3), 334-341 (2010).
54. Stoppe, C., et al. AepEX monitor for the measurement of hypnotic depth in patients undergoing balanced xenon anaesthesia. *Br J Anaesth*. **108** (1), 80-88 (2012).
55. Huang, M. X., et al. Commonalities and Differences among Vectorized Beamformers in Electromagnetic Source Imaging. *Brain Topography*. **16** (3)k 139-158 (2004).
56. Bastos, A. M., & Schoffelen, J.-M. A Tutorial Review of Functional Connectivity Analysis Methods and Their Interpretational Pitfalls. *Frontiers in systems neuroscience*. **9** (January), 175 (2015).
57. Bazanova, O. M., Nikolenko, E. D., & Barry, R. J. Reactivity of alpha rhythms to eyes opening (the Berger effect) during menstrual cycle phases. *International Journal of Psychophysiology*. September 2015, 0-1 (2017).
58. Schaefer, M. S., et al. Predictors for postoperative nausea and vomiting after xenon-based anaesthesia. *Br J Anaesth*. **115** (1), 61-67 (2015).
59. Gan, T. J., et al. Consensus guidelines for the management of postoperative nausea and vomiting. *Anesthesia and Analgesia*. **118** (1), 85-113 (2014).
60. De Vasconcellos, K., & Sneyd, J. R. Nitrous oxide: Are we still in equipoise? A qualitative review of current controversies. *Br J Anaesth*. **111** (6), 877-885 (2013).
61. Sanders, R. D., Ma, D., & Maze, M. Xenon: Elemental anaesthesia in clinical practice. *British Medical Bulletin*. **71**, 115-135 (2004).
62. da Silva, R. M. Syncope: Epidemiology, etiology, and prognosis. *Frontiers in Physiology*. **5** (DEC), 8-11 (2014).
63. Dittrich, A., Lamparter, D., Maurer, M. 5D-ASC: Questionnaire for the assessment of altered states of consciousness. *A short introduction*. (2010).
64. Studerus, E., Gamma, A., & Vollenweider, F. X. Psychometric evaluation of the altered states of consciousness rating scale (OAV). *PLoS ONE*. **5** (8) (2010).
65. Oostenveld, R., Fries, P., Maris, E., & Schoffelen, J. M. FieldTrip: Open source software for advanced analysis of MEG, EEG, and invasive electrophysiological data. *Computational Intelligence and Neuroscience*. **2011** (2011).
66. Stolk, A., Todorovic, A., Schoffelen, J. M., & Oostenveld, R. Online and offline tools for head movement compensation in MEG. *NeuroImage*. **68**, 39-48 (2013).
67. Cimenser, A., et al. Tracking brain states under general anesthesia by using global coherence analysis. *Proc Natl Acad Sci*. **108** (21), 8832-8837 (2011).
68. Hall, S. D., et al. GABA(A) alpha-1 subunit mediated desynchronization of elevated low frequency oscillations alleviates specific dysfunction in stroke - A case report. *Clinical Neurophysiology*. **121** (4), 549-555 (2010).
69. Hall, S. D., et al. The role of GABAergic modulation in motor function related neuronal network activity. *NeuroImage*. **56** (3)(1506-1510 (2011).
70. Cornwell, B. R., et al. Synaptic potentiation is critical for rapid antidepressant response to ketamine in treatment-resistant major depression. *Biological Psychiatry*. **72** (7)(555-561 (2012).
71. Saxena, N., et al. Enhanced Stimulus-Induced Gamma Activity in Humans during Propofol-Induced Sedation. *PLoS ONE*. **8** (3) 1-7 (2013).
72. Quaedflieg, C. W. E. M., Munte, S., Kalso, E., & Sambeth, A. Effects of remifentanyl on processing of auditory stimuli: A combined MEG/EEG study. *J Psychopharmacol*. **28** (1), 39-48 (2014).
73. Muthukumaraswamy, S. D., Shaw, A. D., Jackson, L. E., Hall, J., Moran, R., & Saxena, N. Evidence that Subanesthetic Doses of Ketamine Cause Sustained Disruptions of NMDA and AMPA-Mediated Frontoparietal Connectivity in Humans. *J Neurosci*. **35** (33), 11694-11706 (2015).
74. Bruhn, J., Myles, P. S., Sneyd, R., & Struys, M. M. R. F. Depth of anaesthesia monitoring: What's available, what's validated and what's next? *Br J Anaesth*. **97** (1), 85-94 (2006).
75. Punjasawadwong, Y., Phongchiewboon, A., & Bunchungmongkol, N. Bispectral index for improving anaesthetic delivery and postoperative recovery (Review) Bispectral index for improving anaesthetic delivery and postoperative recovery. *Cochrane Library*. **10**, 10-12 (2010).
76. Taulu, S., Kajola, M., & Simola, J. Suppression of interference and artifacts by the Signal Space Separation Method. *Brain Topography*. **16** (4), 269-75 (2004).
77. Purdon, P.L., et al. Electroencephalogram signatures of loss and recovery of consciousness from propofol. *Proc Natl Acad Sci U S A*. **110** (12), 1142-1151 (2013).
78. Mhuircheartaigh, R.N., et al. Cortical and Subcortical Connectivity Changes during Decreasing Levels of Consciousness in Humans: A Functional Magnetic Resonance Imaging Study using Propofol. *J Neurosci*. **30** (27), 9095-9102 (2010).
79. Pandit, J.J., et al. 5th National Audit Project (NAP5) on accidental awareness during general anaesthesia: summary of main findings and risk factors. *Br J Anaesth*. **113** (4), 549-559 (2014).
80. Lakhan, S. E., Caro, M., & Hadzimichalis, N. NMDA Receptor Activity in Neuropsychiatric Disorders. *Frontiers in Psychiatry*. **4** (June) 52 (2013).